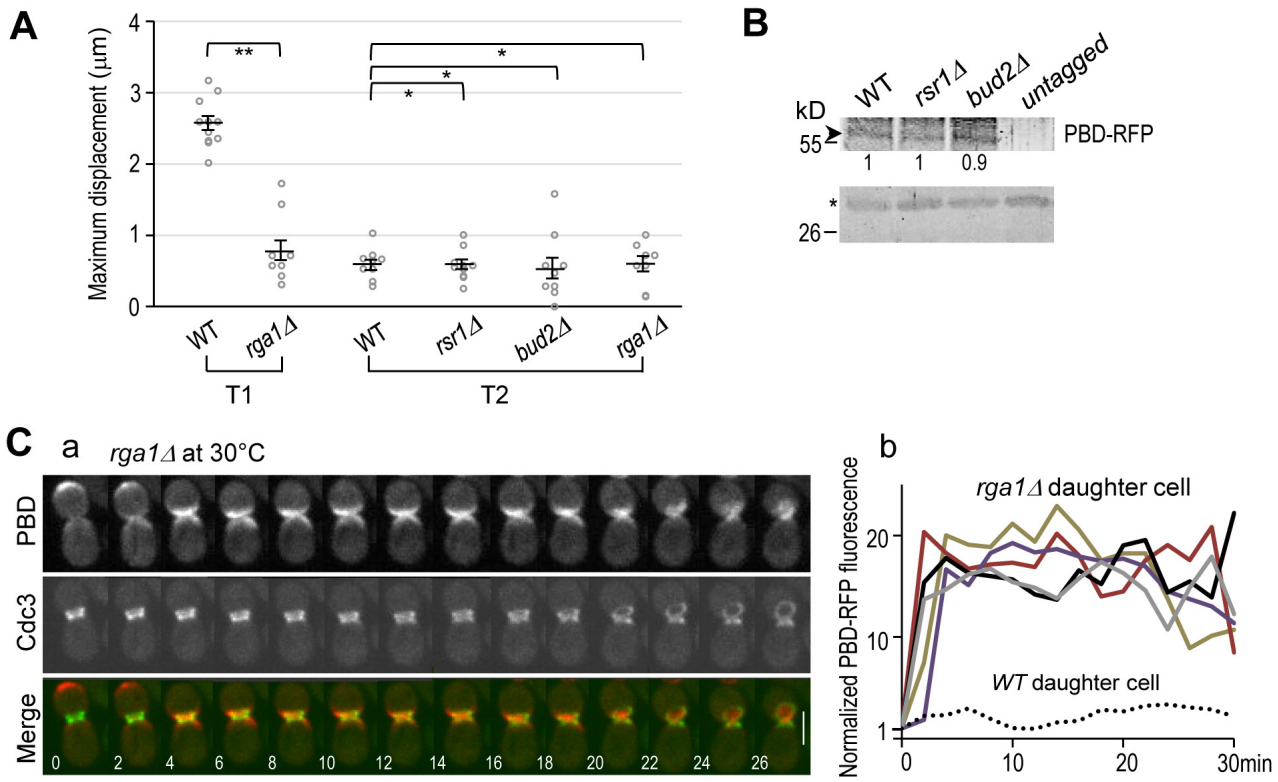

FIG. S1. Analyses of Cdc42-GTP clusters

A. The maximum displacement of the Cdc42-GTP peak in each individual daughter cell of *WT*, *rsr1Δ*, *bud2Δ*, and *rga1Δ* during T1 and T2 (n = 10 cells for each sample). Mean (horizontal lines) ± s.e.m. (error bars) (μm). (*P > 0.7; **P < 10^{-8}). Because of the weak activation of Cdc42 in *rsr1Δ* and *bud2Δ* cells during T1, the displacement is not determined for these mutants (see text for details).

B. The Gic2-PBD-RFP protein level in *WT*, *rsr1Δ*, and *bud2Δ* cells. The relative amounts (numbers below; normalized to the value in *WT*) were estimated using a non-specific cross-reacting band (marked with an asterisk in lower panel) as a loading control.

C. (a) Time-lapse images of PBD-RFP and Cdc3-GFP in *rga1Δ* cells at 30°C. (b) The intensity of the Cdc42-GTP clusters in the bud neck region was normalized to the same at t = 0, and five representative plots are shown in comparison to a representative plot of *WT* cells (a dotted line), which was taken from our previous analysis (Kang et al., 2014). Size bar, 3 μm.

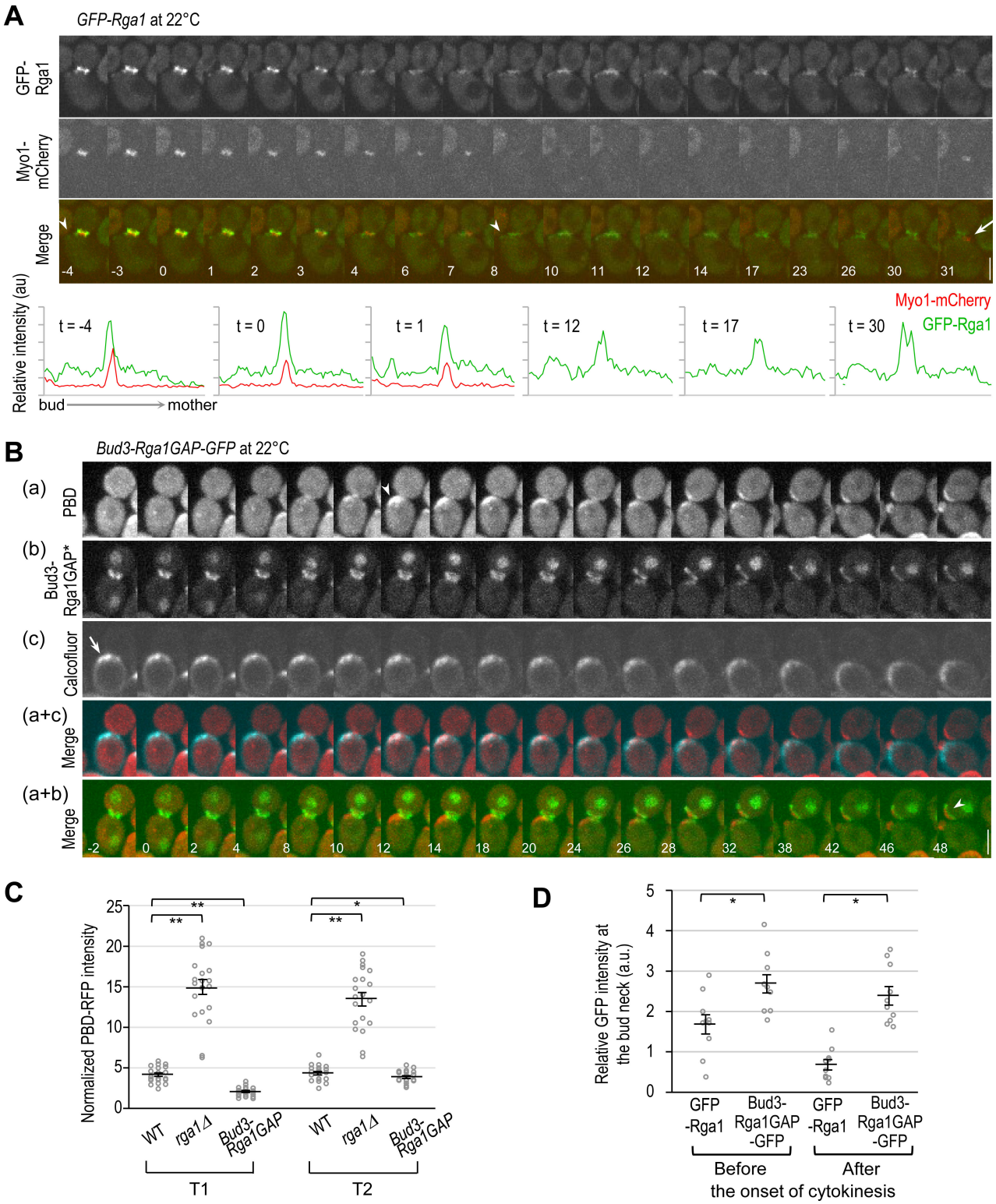

FIG. S2. Localization of Rga1 and Bud3-Rga1GAP

A. Time-lapse analysis of GFP-Rga1 and Myo1-mCherry at 22°C. Arrowheads mark GFP-Rga1 localized to the side of the bud neck before and after the Myo1 ring contraction; and an arrow marks the new Myo1-mCherry. (Below) Line-scan graphs show fluorescence intensities (au) of GFP-Rga1 and Myo1-mCherry along the bud-mother axis at selected time points. Bar, 3 μm.

B. Localization of (a) PBD-RFP; (b) Bud3-Rga1GAP-GFP & Whi5-GFP in an *rga1Δ* cell stained with (c) Calcofluor at 22^{o}C. Merged images are shown below: (a + c) PBD-RFP (red) and Calcofluor (cyan); (a + b) Bud3-Rga1GAP-GFP & Whi5-GFP (green) and PBD-RFP (red). A Cdc42-GTP cluster (marked with an arrowhead) developed at an old bud site (stained with Calcofluor; marked with an arrow) in the mother cell, while a Cdc42-GTP cluster developed within the Bud3-Rga1GAP ring in the daughter cell (marked with an arrowhead at t = 48). Numbers indicate time (in min) from the onset of cytokinesis (t = 0), which was estimated by the appearance of Whi5 to the nucleus (t = -2 or -4). Bar, 3 μm.

C. Quantification of the Cdc42-GTP clusters in daughter cells of *WT*, *rga1Δ,* and *rga1Δ BUD3-RGA1GAP* in T1 and T2 phases. PBD-RFP intensity was normalized to its value at t = 0, and the peak values in each phase are plotted as in Fig. 2Db, except that the bud neck region was used for quantification for all strains. Means (horizontal lines) ± s.e.m. (error bars). (*P = 0.08; **P < 10^{-8}).

D. Fluorescence intensity of GFP-Rga1 and Bud3-Rga1GAP-GFP at the mother–bud neck from individual cells was plotted (n = 10 for each strain). Mean (horizontal lines) ± s.e.m. (error bars). (*P < 0.007).

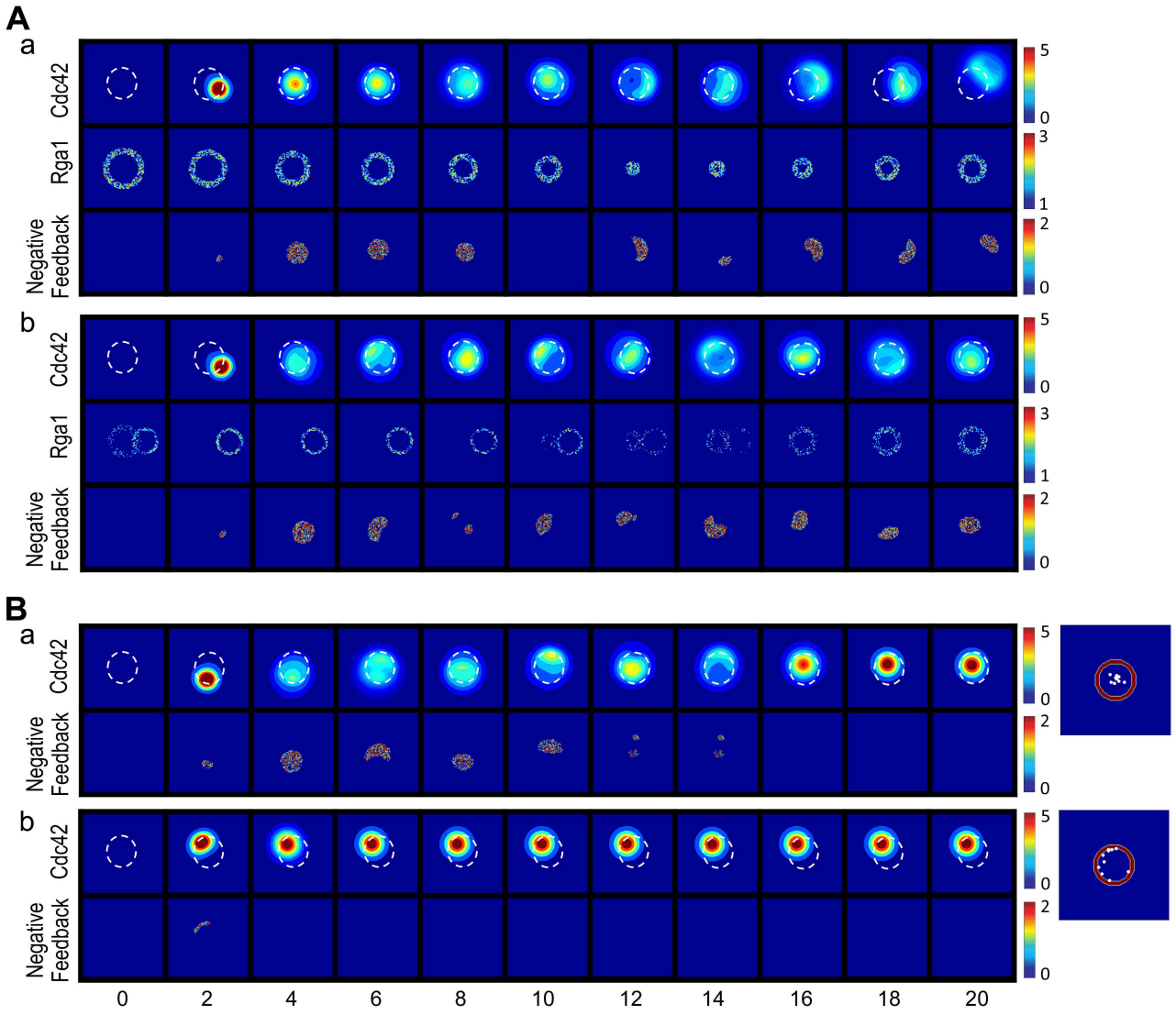

FIG. S3. Computer simulations of Cdc42 polarization with different settings
A. Permanent delayed negative feedback, along with the time-dependent Rga1 localization as observed in (a) daughter cells or (b) mother cells.

B. Delayed negative feedback is assumed only in the first phase and without Rga1 activity: (a) represents the case for daughter cells, in which the first phase is assumed to last for 15 min; and (b) represents the case for mother cells, in which the first phase is assumed to last for 3 min. Numbers below panel **B** denote time (min) from cell division.

(Right panels) Positions of maximum Cdc42-GTP after 20 min in 10 different simulations for the corresponding case from **B**. The axial landmark is depicted as a red ring.

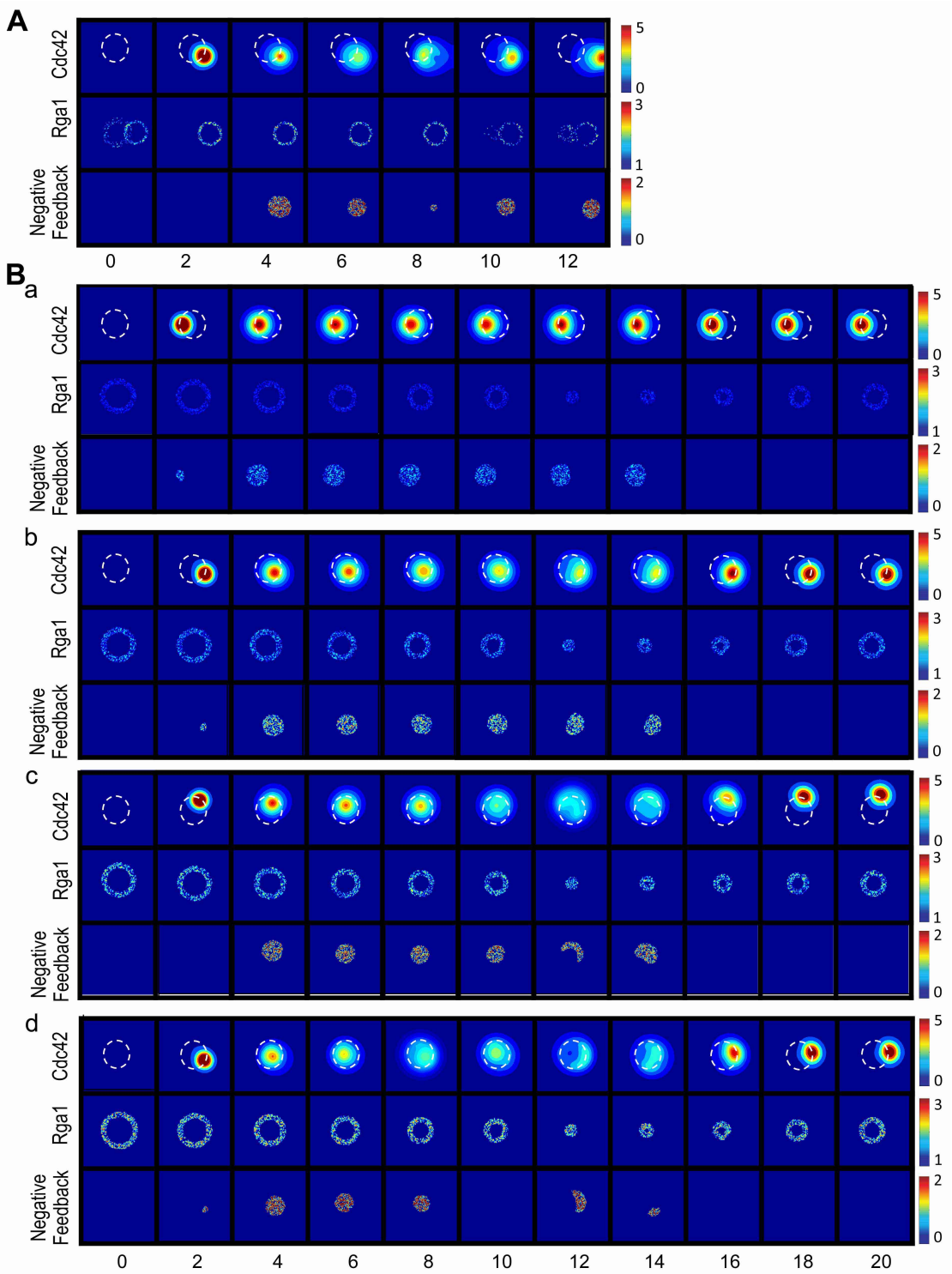

FIG. S4. Computer simulations of Cdc42 polarization for additional controls

A. Simulations for mother cells when the first and second phases are reversed from the case shown in Fig. 7Bb. See also legend to Fig. 7Bb.

B. Simulations for daughter cells with different Rga1 signal strengths. The maximum of Rga1 signal strength is assumed as follows: a) 1.5 min^{-1}, b) 2 min^{-1}, c) 2.5 min^{-1}, and d) 3 min^{-1}. Other parameters are the same as in Fig. 7Ba. See legend to Fig. 7Ba.

Movie 1. **Localization of Cdc42-GTP in *rsr1Δ* cells.** Gic2-PBD-tdTomato (left), Cdc3-GFP (middle), and merge (right) are shown from time-lapse images of haploid *rsr1Δ* cells. Images were captured at 2 min intervals using a spinning-disk confocal microscope at 30°C. The video shows frames for 34 min starting from 4 min before the onset of cytokinesis**.** Display rate is 8 frames/sec**.** Selected images are shown in Fig. 2A.

Movie 2. **Localization of GFP-Rga1 and Cdc3-mCherry in haploid *WT* cells.** GFP-Rga1 (left), Cdc3-mCherry (middle), and merge (right) are shown from time-lapse images of *WT* cells. Images were captured at 2-min intervals using a spinning-disk confocal microscope at 22°C. The video shows frames for 56 min, starting from 4 min before the onset of cytokinesis. Display rate is 8 frames/sec. Selected images are shown in Fig. 5A.

Table S1. Duration times of T1 and T2 in mother (M) and daughter (D) cells

	WT	***rsr1Δ***	***bud2Δ****	***rga1Δ***	***rga1Δ BUD3 -RGA1GAP***
T1 in M cells	6.67 ± 0.67 (12)	5.80 ± 0.76 (10)	19.9 ± 1.43 (20)	5.46 ± 0.36 (15)	6.60 ± 0.85 (10)
T2 in M cells	14.36 ± 0.65 (11)	15.67 ± 0.61 (6)		14.93 ± 1.18 (15)	13.40 ± 1.90 (10)
T1 in D cells	26.00 ± 2.27 (7)	26.67 ± 5.12 (9)	39.1 ± 3.20 (17)	26.57 ± 1.79 (14)	26.00 ± 2.57 (9)
T2 in D cells	14.86 ± 0.40 (7)	14.33 ± 0.33 (6)		15.00 ± 0.68 (10)	12.89 ± 0.95 (9)

Numbers indicate the mean ± s.e.m. (min) of T1 and T2, which were estimated by the nuclear exit of Whi5-GFP. Total cell number is shown in ( )**.**

*Numbers in *bud2Δ* cells indicate estimated time for T1 plus T2 (from the onset of cytokinesis until bud emergence).

Table S2. Yeast strains used in this study

Strain		Relevant Genotype[a]	Source
YEF473A	*MAT***a**	*his3-Δ200 leu2-Δ1 lys2-801 trp1-Δ63 ura3-52*	(Bi and Pringle, 1996)
YZT292	*MAT***a**	*CDC3-GFP::LEU2 GIC2-PBD-tdTomato::URA3*	(Tong et al., 2007)
YZT293	*MAT***a**	*rga1Δ::HIS3 CDC3-GFP::LEU2 GIC2-PBD-tdTomato::URA3*	(Tong et al., 2007)
YEF2324	*MAT***a**	*rga1Δ::HIS3*	(Tong et al., 2007)
JGY1622	*MAT***a**	*rga1Δ::HIS3 BUD3-rga1(aa700–1007)-GFP:URA3*	(Tong et al., 2007)
YZT158	*MAT***a**	*GFP-RGA1*	(Tong et al., 2007)
HPY2512	*MAT***a**	*GFP-RGA1 CDC3-mCherry::LEU2*	This study
HPY2671	*MAT*α	*WHI5-GFP::TRP1 GIC2-PBD- tdTomato::URA3*	This study[b, e]
HPY2690	*MAT***a**	*BUD3-rga1(aa700–1007)-GFP::URA3*	This study[d]
HPY2653	*MAT*α	*rsr1Δ::URA3 CDC3-GFP::LEU2 GIC2-PBD-tdTomato::URA3*	This study[b]
HPY2626	*MAT***a**	*rga1Δ::HIS3 BUD3-rga1(aa700–1007)-GFP:URA3 WHI5-GFP::TRP1 GIC2-PBD^{W23A}-tdTomato::LEU2*	This study[c]
HPY2669	*MAT*α	*rsr1Δ::URA3 WHI5-GFP::KANMX6 GIC2-PBD-tdTomato::URA3*	This study[b, e]
HPY2695	*MAT***a**	*bud2Δ::LEU2 CDC3-GFP::LEU2 GIC2-PBD-tdTomato::URA3*	This study[b]
HPY2668	*MAT*α	*rga1Δ::HIS3 WHI5-GFP::TRP1 GIC2-PBD-tdTomato::URA3*	This study[b]

[a]All strains are isogenic to YEF473A, except as indicated. The original strains and plasmids expressing Gic2-PBD-tdTomato, GFP-Rga1, Bud3-Rga1GAP-GFP, and Cdc3-mCherry were previously described (Tong et al., 2007). Plasmid pRS314-MYO1-mCherry (Wloka et al., 2011) was transformed into YZT158 for imaging.

[b]YIp211-GIC2-PBD(aa 1-208)-tdTomato (Tong et al., 2007) was used for integration at the *ura3* locus.

[c]YIplac128-PBD^{W23A}-tdTomato (Okada et al., 2013) was used for integration at the *leu2* locus.

[d]The Bud3-Rga1GAP-GFP fusion was expressed in haploid *WT* (HPY210) at the *BUD3* locus by targeting the Rga1GAP domain (aa 700-1007) (which was fused to GFP) into the 3' of the *BUD3* ORF. Expression of Bud3-Rga1GAP-GFP did not interfere the axial budding pattern of *WT* (*RGA1*) haploid cells (data not shown).

[e]Whi5-GFP was expressed by targeting GFP at the C terminus, replacing the endogenous Whi5 (Kang et al., 2014).

Table S3. The values of parameters used in the simulations

Parameters	Value*	References
D_m	$0.1\mu m^2\,\mathrm{min}^{-1}$	(Goryachev and Pokhilko, 2008; Lo et al., 2013)
K_1	0.3	(Lo et al., 2013) & estimated
K_2	0.2	(Lo et al., 2013) & estimated
k_{on1}, k_{on2}	$1\,\mathrm{min}^{-1}$	(Lo et al., 2013) & estimated
K_{off}	2	This study
t_1	1 min	This study
t_{off}	a) 15min (daughter cells) b) 3min (mother cells) S3A infinity	This study

* The value of the normalizing parameter K_1 was chosen to achieve spontaneous budding without spatial cues. The parameter K_{off} is the threshold of Cdc42 for functioning negative feedback and t_1 is the time delay for negative feedback. This setting is based on the best simulation for achieving dynamic movement of Cdc42-GTP cluster. We observed that the conclusion obtained from the outputs is consistent when K_{off} is between 1 and 3 and t_1 is between 0.75 min and 1.5 min. In the Figures, (a) and (b) represents the case for haploid daughter cells (*i.e.*, t_{off} = 15 min) and mother cells (*i.e.*, t_{off} = 3 min), respectively.

Table S4. Formula for the deactivation term and specific settings used in the simulations

$$k_{off}(a(x,t-t_1),x,t) = g_1(x,t) + g_2(x,t)H(a(x,t-t_1)-K_{off}),\ \ H(a) = \begin{cases} 0, \text{ if } a \le 0 \\ 1, \text{ if } a > 0 \end{cases}.$$

Figures	$g_1(x,t)$ (Rga1-mediated deactivation)	$g_2(x,t)$ (negative feedback on the deactivation)
4B	$1\,\text{min}^{-1}$	$0\,\text{min}^{-1}$
4C	$1\text{min}^{-1}+2d_d(x,t)$* if $0.5<\|x\|<0.65$; 1min^{-1} otherwise	$0\,\text{min}^{-1}$
7A	Rga1 dynamics shown in Fig. 7A**	$0\,\text{min}^{-1}$
7B	Rga1 dynamics shown in Fig. 7B**	$4\theta_1(t)\delta_d(x)$
7C	$1\text{min}^{-1}+2d_d(x,t)$ if $0.5<\|x\|<0.65$; 1min^{-1} otherwise	$4\theta_1(t)\delta_d(x)$
S3A	Rga1 dynamics shown in Fig. 7A	$4\delta_d(x)$
S3B	$1\,\text{min}^{-1}$	$4\theta_1(t)\delta_d(x)$

* $_d(x,t)$ is a spatiotemporal uncorrelated random function with uniform distribution between 0 and 1 for each x and t.

**The distribution of Rga1 changes according to the following formula for the changes of the non-zero regions (r is the distance from a point to the center of the domain, namely ($|x|$); r' is the distance from a point to the point 1mm right to the center of the domain, namely ($|x-(1,0)|$)):

Daughter cells: $\{0.3(1-t/10)+0.3<r<0.3(1-t/10)+0.6\}$ for $0<t$ 10; $\{r<0.3\}$ for $10<t$ 12; $\{0.35(t-12)/8<r<0.35(t-12)/8+0.3\}$ for $12<t$ 20;

Mother cells: $\{0.5<r<0.8\}$ and $\{0.5<r'<0.65\}$ for $0<t$ 2; $\{0.5<r'<0.65\}$ for $2<t$ 8; $\{0.35(t-16)/8<r<0.35(t-16)/8+0.3\}$ and $\{0.5<r'<0.65\}$ for $8<t$ 16; $\{0.35<r<0.65\}$ for $16<t$ 20.

The results in Fig. S4, B show that when the maximum of Rga1 signal strength increases to 3min^{-1}, the Cdc42 localization becomes more drifting. To match with experimental observation, we take the maximum of Rga1 signal to be 3min^{-1} and the magnitude of Rga1 $3d_d(x,t)$. Note that the negative feedback functions when $a(x,t-t_1)$ is larger than K_{off}.